Timing Jitter in a Long-Haul 40 Gb/s Dispersion-Managed Soliton System

R. Holzlöhner,[1] H. N. Ereifej,[2] G. M. Carter,[1,2] and C. R. Menyuk[1,3]

[1] *Department of Computer Science and Electrical Engineering,*
University of Maryland Baltimore County,
TRC 201 B, 1000 Hilltop Circle, Baltimore, MD 21250
tel: 410-455-3318, fax: 410-455-6500, email: holzloehner@umbc.edu
http://www.photonics.umbc.edu/

[2] *Laboratory for Physical Sciences, College Park, MD 20740*

[3] *PhotonEx Corporation, 200 MetroWest Technology Park, Maynard, MA 01754*

Abstract: We show by careful comparison between experiment and simulation of a 40 Gb/s dispersion-managed soliton (DMS) system that the error-free transmission distance is limited to 6,300 km by both Gordon-Haus and inter-symbol induced timing jitter.

OCIS codes: (060.0060) Fiber optics communications

1 Introduction

Increasing the data rate in optical transmission systems from 10 Gb/s to 40 Gb/s poses many challenges. Both experiments and numerical simulations face new problems that require a detailed understanding of the system limitations. Physical effects that were already present at 10 Gb/s, but could be neglected, have to be taken into account at 40 Gb/s. The error-free optical transmission of the signal becomes more complicated to achieve. First, pulses are usually shorter, so that the optical bandwidth is larger than at 10 Gb/s and hence solitons interact more strongly with ASE noise. Second, as a consequence of the reduced pulse spacing, inter-symbol interference (ISI) typically becomes more severe [1]. The tolerance of the system performance to variation of parameters such as path average dispersion, amplifier location, filter bandwidth, and optical power is much smaller than at 10 Gb/s.

We present an experimental and numerical study of a dispersion-managed soliton (DMS) system at both 10 Gb/s and 40 Gb/s. The system consists of a recirculating loop of length 106 km. The major detrimental effects that limit the achievable transmission distance are timing and amplitude jitter. Our key result is that both amplitude and timing jitter increase at 40 Gb/s due to ISI. This problem is serious since the receiver's tolerance for timing jitter in a 40 Gb/s system is only about 1.5 ps, down from 5.5 ps at 10 Gb/s [2].

2 Experimental setup and results

The recirculating loop setup contained four dispersion map periods with a combined length of 106 km. Each map period comprised a normal span 25 km long with dispersion −1.02 ps/nm-km and an anomalous span 1.53 km long with dispersion 17 ps/nm-km. The path average dispersion was in the range 0.005–0.025 ps/nm-km, depending on the central wavelength of the signal, and the dispersion slope was 0.0768 ps^2/nm-km. Each map contained an EDFA that divided the normal span into pieces of 19.6 km and 5.38 km respectively. This location minimizes pulse stretching and hence ISI. The fourth map contained a 3.8 nm optical bandpass filter to reduce the noise, and its anomalous span was split in half, with a fifth EDFA, an AO loop switch, and the 3 dB-coupler inserted in the middle. A 10 GHz train of pulses, each pulse with a pulse width of 4.5 ps, was modulated with a $2^{23}-1$ pseudorandom sequence at 10 Gb/s using a $\mathrm{LiNbO_3}$ intensity modulator. The signal was multiplexed by a two-stage optical multiplexer. The unchirped signal then passed the coupler and was inserted into the loop with a peak power of 7.6 mW. The pulses had a Gaussian shape and reach an equilibrium pulse width of 6 ps during propagation measured at the transform limit point in the map. The average optical power was 1.5 dBm at 40 Gb/s and −3.5 dBm at 10 Gb/s. Peak power and pulse width are approximately identical at both bit rates. At the receiver, the 40 Gb/s data was optically demultiplexed back to 10 Gb/s for eye diagram and error rate measurements.

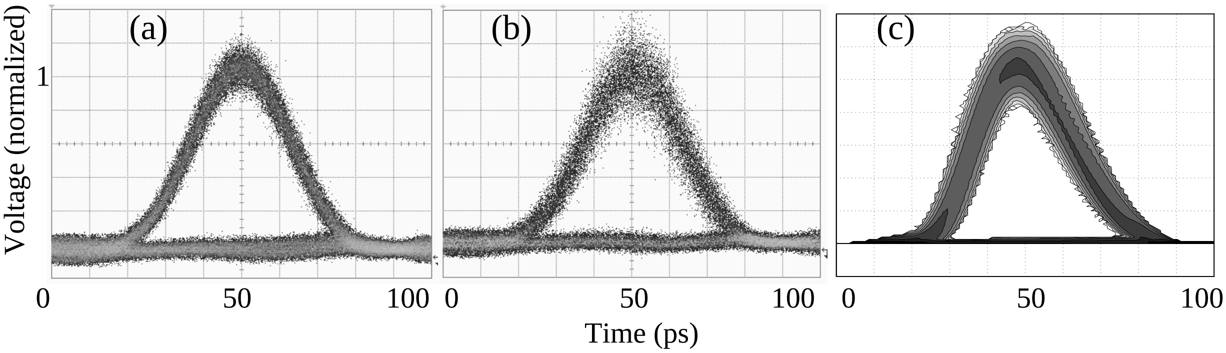

Fig. 1. Eye diagram of a pulse demultiplexed from a 40 Gb/s data stream at the output of a 20 GHz photodiode, (a) back-to-back and (b) after propagating 6,000 km. (c) Simulated eye diagram. The slightly asymmetrical pulse shape is due to the electrical model of the bandwidth-limited photodiode.

We use the scalar split-step method to simulate the light propagation in a time window of 3.2 ns, containing 128 bits at 40 Gb/s and 32 bits at 10 Gb/s. In the recirculating loop that we are modeling, the polarization dependent loss is about 0.35 dB per round trip and the polarization controllers are optimized to pass the signal with minimum loss, yielding a degree of polarization greater than 0.95. Consequently, the orthogonal polarization is suppressed. We run Monte Carlo simulations in which a different bit sequence is chosen for each realization; the ratio of marks and spaces is always 1:1. The EDFAs are modeled as saturable amplifiers with a saturation time of 1 ms and a saturation power of 10 mW. Details on the simulation procedure can be found in [3]. The spontaneous emission factor is $n_{\mathrm{sp}} = 1.2$. At the receiver, we carefully model the optical demultiplexer with realistic window functions, clock recovery circuit, bandwidth limited photodiode, and narrow-band electrical filter with a bandwidth of 8.6 GHz. We note that proper receiver modeling becomes more critical as we go from 10 Gb/s to 40 Gb/s. For example, our photodiode broadens the received pulses from 6 ps to 23–30 ps and hence has a major influence on the eye diagram. This broadening was not important in previous 10 Gb/s experiments [3]. We model the effective demultiplexer transmission window using a Butterworth function $f(t) = 1/[1 + |2(t - t_0)/T_{\mathrm{FWHM}}|^k]$, where t is time, t_0 the central time of the window, $T_{\mathrm{FWHM}} = 26$ ps the window duration, and $k = 6.5$.

Fig. 1 shows eye diagrams from a 40 Gb/s data stream demultiplexed down to 10 Gb/s directly at the output of the photodiode, before narrow-band filtering. Plots (a) and (b) show the eye diagram of a single pulse at 0 km and 6,000 km respectively. Plot (c) is a simulated eye diagram in the form of a contour plot, where contours follow lines of constant trace density. Fig. 2(a) shows the timing jitter evolution of the 40 Gb/s and the 10 Gb/s experiments, where the curves display the results from the numerical simulation. Due to the absence of pulse overlap, the 10 Gb/s data is a result of Gordon-Haus timing jitter [2]. The jitter growth is almost linear owing to the optical inline filter. By running the experiment with the same pulse parameters at 40 Gb/s we are then able to measure the contribution to the jitter from the nonlinear interaction of adjacent pulses. In the simulation we find that neighboring pulses attract each other, regardless of their initial phase difference. The pulse attraction is reduced by a mere 5% if we alternate the phases of adjacent pulses by π, compared to constant phase. This result is consistent with [4]. The experimental transmission is error-free up to 6,300 km at 40 Gb/s and 12,000 km at 10 Gb/s. We note that the present experiment was optimized for 40 Gb/s. Changing the parameters in this experiment to optimize for 10 Gb/s transmission permits error-free transmission over 18,000 km.

At 40 Gb/s the breakdown of the transmission occurs in two stages. First, at 6,300–7,500 km, timing jitter degrades the received signal so that clock recovery fails. Second, beyond 7,500 km, the pulses themselves break apart. The present system is therefore limited by timing jitter, not by noise in the spaces (zeros) as was the case in our earlier 10 Gb/s experiments [3]. As a consequence, the bandwidth and exact filter profile of the optical inline filter are not as important as in the 10 Gb/s system; we varied filter types and the filter bandwidth between 2.8 nm and 4.6 nm without observing large differences in the maximum transmission distance. We compared the above timing jitter values, which are directly taken from a digital sampling oscilloscope, with a method introduced by Mollenauer [5] that relies on the fading of RF tones with

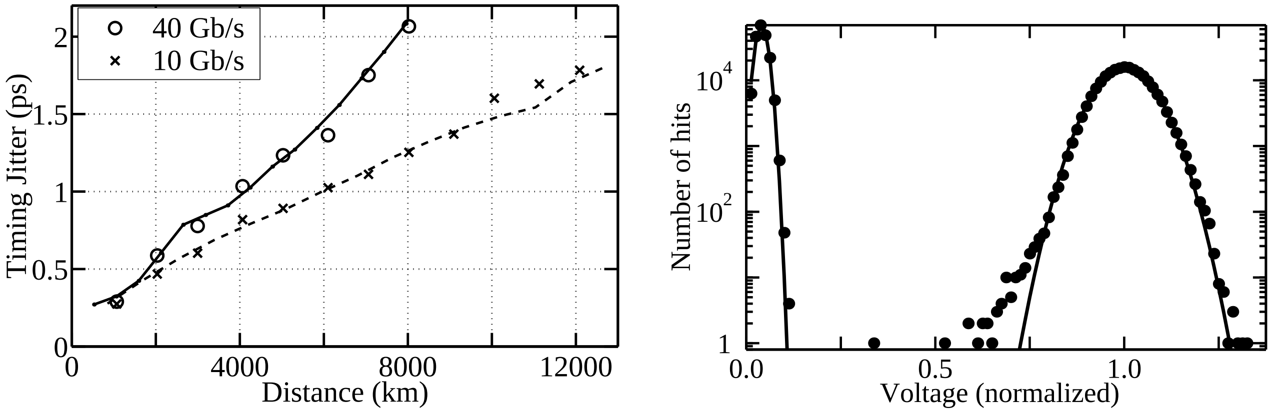

Fig. 2. (a) Timing jitter at 40 Gb/s and 10 Gb/s. The circles and crosses show the timing jitter measured on a digital sampling oscilloscope, the solid and dashed lines are results of the simulation. (b) Histogram of the narrow-band filtered receiver voltage resulting from the Monte Carlo simulation at a propagation distance of 7,500 km. The left peak corresponds to the zeros, the right one to the marks. The solid lines are Gaussian fits. The departure from Gaussian behavior is obvious at low probability densities. Even a Gaussian fit to the tails of the distributions fails.

transmission distance. The results from the RF tone method are smaller by approximately 10% compared to the values in Fig. 2(a) because they are not influenced by amplitude jitter and therefore adhere better to the most commonly used definition of timing jitter, namely the standard deviation of the pulse center offsets in time. Fig. 2(b) shows a histogram of the received voltage after narrow-band filtering, obtained from the Monte Carlo simulation of 3,000 realizations. The propagation distance is 7,500 km which is about 1,200 km beyond the distance where error-free transmission breaks down. The solid lines are Gaussian fits to the data points. The Q-factor based on the Gaussian fits is still larger than 6, indicating error-free transmission. However, due to the departure of the probability density from Gaussian shape, the true error rate exceeds 10^{-9} as is the case in the experiment.

3 Conclusion

We successfully compared experiment and simulation of a 40 Gb/s dispersion-managed soliton (DMS) system in a recirculating loop. We used periodic dispersion compensation and a 3.8 nm optical inline filter. Reducing the data rate to 10 Gb/s, while keeping other parameters constant, we were able to isolate the impact of intersymbol interference (ISI). Timing jitter and ISI are strongly coupled in our loop and limit the propagation distance. Our results demonstrate the increased care that is needed to correctly design and model systems with a single-channel data rate of 40 Gb/s as compared to systems with 10 Gb/s. In particular, we found that path average dispersion, EDFA placement, filter center wavelength, and optical power must be precisely adjusted to optimize transmission. Once we had understood and controlled all the key parameters, we were able to achieve excellent agreement between theory and experiment and error-free propagation over distances of about 6,300 km. Beyond this distance, our simulation shows that the probability distribution of the receiver voltage starts to deviate from a Gaussian shape and hence the Q-factor as a figure of merit becomes unreliable.

References

1. K. Suzuki, H. Kubota, A. Sahara, and M. Nakazawa, "40 Gbit/s single channel optical soliton transmission over 70,000 km using inline synchronous modulation and optical filtering," Electron. Lett. **34,** 98–100 (1998).
2. J. P. Gordon and H. A. Haus, "Random walk of coherently amplified solitons in optical fiber transmission," Opt. Lett. **11,** 665–667 (1986).
3. R.-M. Mu, V. S. Grigoryan, C. R. Menyuk, G. M. Carter, and J. M. Jacob, "Comparison of theory and experiment for dispersion-managed solitons in a recirculating fiber loop," IEEE J. Sel. Topics Quant. Electron. **6,** 248–257 (2000).
4. T. Yu, E. A. Golovchenko, A. N. Pilipetskii, and C. R. Menyuk, "Dispersion-managed soliton interactions in optical fibers," Opt. Lett. **22,** 793–795 (1997).
5. L. F. Mollenauer, M. J. Neubelt, S. G. Evangelides, J. P. Gordon, and L. G. Cohen, "Experimental study of soliton transmission over more than 10,000 km in dispersion-shifted fiber," Opt. Lett. **15,** 1203–1205 (1990).